The Cambrian Conundrum: Early Divergence and Later Ecological Success in the Early History of Animals

Douglas H. Erwin,[1,2]* Marc Laflamme,[1] Sarah M. Tweedt,[1,3] Erik A. Sperling,[4] Davide Pisani,[5] Kevin J. Peterson[6]*

Diverse bilaterian clades emerged apparently within a few million years during the early Cambrian, and various environmental, developmental, and ecological causes have been proposed to explain this abrupt appearance. A compilation of the patterns of fossil and molecular diversification, comparative developmental data, and information on ecological feeding strategies indicate that the major animal clades diverged many tens of millions of years before their first appearance in the fossil record, demonstrating a macroevolutionary lag between the establishment of their developmental toolkits during the Cryogenian [(850 to 635 million years ago Ma)] and the later ecological success of metazoans during the Ediacaran (635 to 541 Ma) and Cambrian (541 to 488 Ma) periods. We argue that this diversification involved new forms of developmental regulation, as well as innovations in networks of ecological interaction within the context of permissive environmental circumstances.

When Charles Darwin published *The Origin of Species* (*1*), the sudden appearance of animal fossils in the rock record was one of the more troubling facts he was compelled to address. He wrote: "There is another and allied difficulty, which is much graver. I allude to the manner in which numbers of species of the same group, suddenly appear in the lowest known fossiliferous rocks" (p. 306). Darwin argued that the incompleteness of the fossil record gives the illusion of an explosive event, but with the eventual discovery of older and better-preserved rocks, the ancestors of these Cambrian taxa would be found. Studies of Ediacaran and Cambrian fossils continue to expand the morphologic variety of clades, but the appearance of the remains and traces of bilaterian animals in the Cambrian remains abrupt (Fig. 1 and tables S1 and S2).

The fossil record is now supplemented with geochemical proxies of environmental change; a precise temporal framework allowing for correlation of rocks in different areas of the world and evaluation of rates of evolutionary and environmental change; an increasingly rigorous understanding of the phylogenetic relationships between various living and fossil metazoan clades and their dates of origin, based largely on molecular sequences; and growing knowledge of the evolution of developmental processes through comparative studies of living groups. Collectively, these records allow an understanding of the environmental potential, genetic and developmental possibility, and ecological opportunity that existed before and during the Cambrian. Here, we provide an updated synthesis (*2*, *3*) of these records and thereby a macroevolutionary framework for understanding the Cambrian explosion.

Pattern of Animal Diversification

The Cambrian fossil record. The beginning of the Cambrian Period dated at 541 ± 0.13 million years ago (Ma) (*4*) is defined by the first appearance of the trace fossil *Treptichnus pedum* (*5*) in the rock record, representing the first appearance of bilaterian animals with the ability to make complex burrows both horizontally (Fig. 2A) and vertically (*6*). The earliest skeletal fossils occur in the latest Ediacaran, but the first appearance of an array of plates, spines, shells, and other skeletal elements of bilaterian affinity begins during the early Cambrian Fortunian Stage (541 to ~530 Ma) (*7*, *8*) (Fig. 3). Most of these are disarticulated elements larger than 2 mm in size, but some complete scleritomes (Fig. 2B) have been recovered. They reveal a fauna with considerable morphologic and phylogenetic diversity and are collectively referred to as the "small shelly fauna" (SSF). The earliest SSF are largely of lophotrochozoan affinities; only in Cambrian Stage 3 do biomineralized ecdysozoans and deuterostomes appear (*8*). Many of the SSF elements are preserved as phosphate minerals, and their diversity peaks in abundant phosphate depos-

its (*9*). Although Ediacaran phosphate deposits are common, they lack SSF, suggesting that bilaterian clades acquired skeletons during the Cambrian.

The pattern seen from the skeletal and trace fossil record is mirrored by soft-bodied fossils found in exceptionally preserved Cambrian faunas in China, Greenland, Australia, Canada (Fig. 2C), and elsewhere. Although many new groups have been described over the past decade, the pattern of diversification of both body fossils and trace fossils has remained largely robust: A recompilation (SOM text 1 and table S1) of the first occurrences of all metazoan phyla, classes, and stem-classes (extinct clades) of equivalent morphologic disparity (Fig. 2, D and E) shows their first occurrences in the latest Ediacaran (by 555 Ma), with a dramatic rise over about 25 million years in the first several stages of the Cambrian, and continuing into the Ordovician (Figs. 1 and 3 and table S3). However, from the early Paleozoic onward there is little addition of new phyla and classes (Fig. 1), and those that are added are largely artifactual, as they represent occurrences of taxa with little or no preservation potential (*10*).

The molecular record. Given the clear signal for an explosive appearance of animal fossils in the early Cambrian (Figs. 1 and 3), most paleontologists favor a near literal reading of the fossil record, supporting a rapid (~25-million-year) evolutionary divergence of most animal clades near the base of the Cambrian [e.g., (*11*)]. But teasing apart the mechanisms underlying the Cambrian explosion requires disentangling evolutionary origins from geological first appearances, and the only way to separate the two is to use a molecular clock (*12*). Many earlier problems with molecular divergence estimates have been addressed, allowing confident estimates of the robustness of the known geologic record (*13*, *14*).

Building upon a previously assembled data set (*14*) and a generally accepted phylogenetic tree, we estimated divergence times for >100 species of animals (alignment available as database S1), encompassing all major metazoan clades (Fig. 1, SOM text 2, table S4, figs. S1 to S4, and database S2). Although much of the topology is well accepted, including the tripartite division of bilaterians into lophotrochozoans, ecdysozoans, and deuterostomes and the paraphyletic nature of "diploblasts" with respect to triploblasts (*15–17*), the paraphyletic nature of sponges is more controversial (*15*, *17*). However, the estimated divergence times (SOM text and figs. S5 to S10) do not depend on this presumption; they are also robust to the choice of the root prior, the molecular clock model, subsampling of the calibration points, and relaxation of the bounds of the calibration point intervals themselves (table S4). Although acoelomorphs have figured prominently in discussions about the reconstruction of ancestral bilaterians (*18*, *19*), they are not included in

[1]Department of Paleobiology, MRC-121, National Museum of Natural History, Post Office Box 37012, Washington, DC 20013–7012, USA. [2]Santa Fe Institute, 1399 Hyde Park Road, Santa Fe, NM 87501, USA. [3]Behavior, Ecology, Evolution and Systematics, University of Maryland, College Park, MD 20742, USA. [4]Department of Earth and Planetary Sciences, Harvard University, Cambridge, MA 02138, USA. [5]Department of Biology, The National University of Ireland, Maynooth, Kildare, Ireland. [6]Department of Biology, Dartmouth College, Hanover, NH 03755, USA.

*To whom correspondence should be addressed. E-mail: erwind@si.edu (D.H.E); kevin.j.peterson@dartmouth.edu (K.J.P.)

the analysis owing to their incomplete gene sampling and very long branches; moreover, a recent analysis (20) indicates that they may be derived deuterostomes, and thus their only contribution to this analysis would be to demonstrate the extent of character loss among some bilaterian clades (see below).

These molecular estimates suggest that the origin and earliest diversification of animals occurred during the Cryogenian Period. We estimate that the last common ancestor of all living animals arose nearly 800 Ma and that the stem lineages leading to most extant phyla had evolved by the end of the Ediacaran (541 Ma). Most

phylum-level crown group divergences occurred coevally between the end of the Ediacaran and the end of the Cambrian (Figs. 1 and 3, large colored circles). This is the case both for taxa with robust fossil records (e.g., echinoderms, molluscs, arthropods) and those with sparse fossil records (e.g., nemerteans, nematodes). For
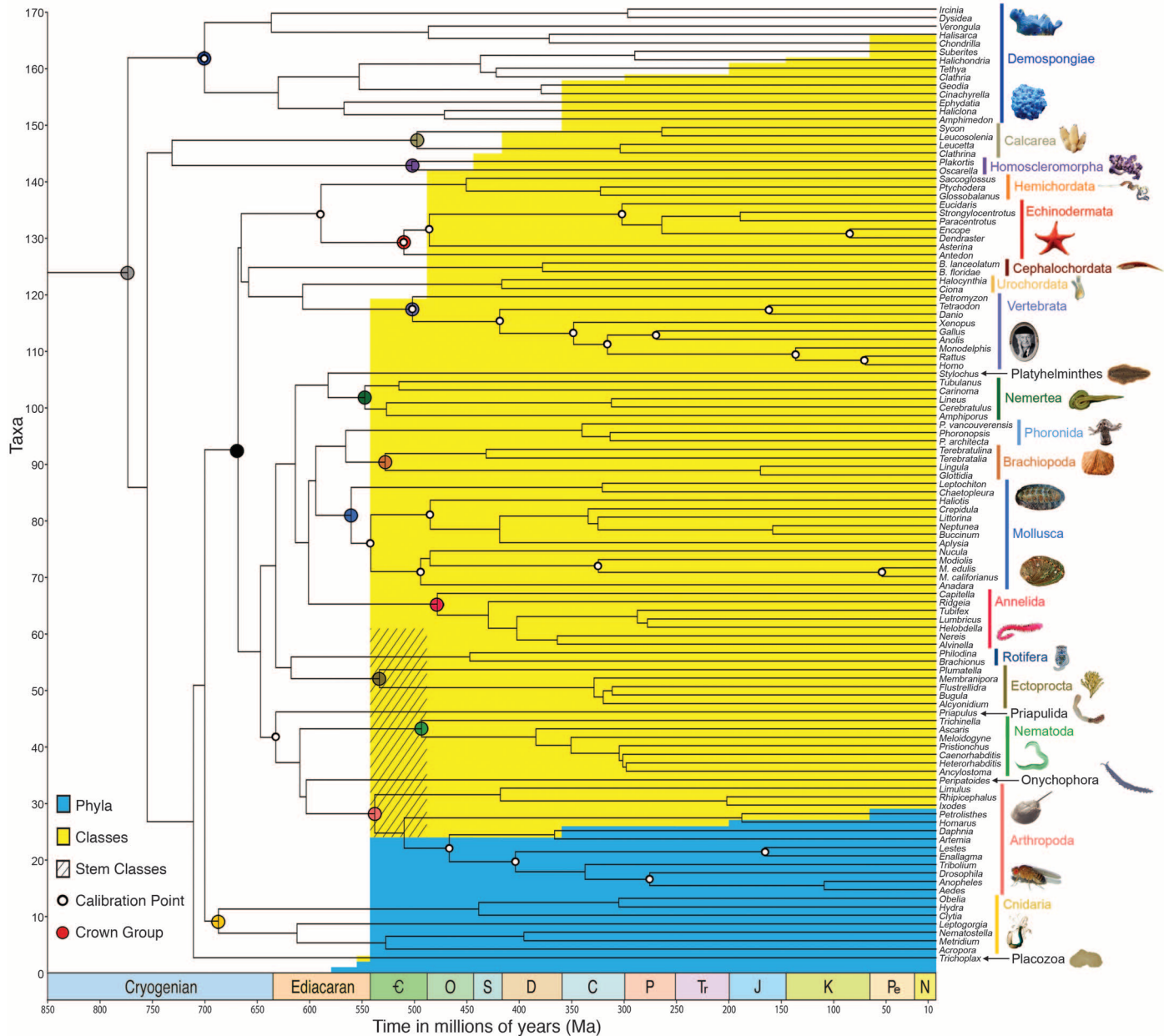
Fig. 1. The origin and diversification of animals as inferred from the geologic and genetic fossil records. The dramatic rise in the number of animal fossils (see scale on left) in the Cambrian relative to the Ediacaran conveys the impact of the Cambrian explosion of animal life. Little high-level morphological innovation occurred during the subsequent 500 million years in that much of animal disparity, as measured by the Linnean taxonomic ranking, was achieved early in the radiation. Overlying the geologic record is the pattern of animal origination as inferred from the molecular clock. Seven different housekeeping genes from 118 taxa were used to generate this chronogram (see SOM 2 for methodological details and database S1). Twenty-four calibrations (open circles) were used and treated as soft bounds. Divergence times for key nodes and their 95% highest posterior intervals are reported in data-base S2. All estimates appear to be robust to numerous experimental manipulations performed to assess whether the results were dependent on the parameters used in the analyses (Materials and Methods, SOM Text 2, and figs. S5 to S10). There is general concordance of bilaterian phylum-level crown groups (colored circles; the color of each circle is the same as the corresponding taxonomic bar and label on the far right), with the first appearance of most animal groups at the Ediacaran-Cambrian boundary. In contrast, the origins of the demosponge (dark blue) and cnidarian (yellow) as well as the bilaterian (black) and metazoan (gray) crown groups are deep in the Cryogenian. Geological period abbreviations: Є, Cambrian; O, Ordovician; S, Silurian; D, Devonian; C, Carboniferous; P, Permian; Tr, Triassic; J, Jurassic; K, Cretaceous; Pe, Paleogene; N, Neogene. A high-resolution image is available in the SOM.

taxa with robust fossil records, these coeval origination estimates are concordant with their first appearances in the rock record (Fig. 3), supporting both the general accuracy of our relaxed molecular clock analysis and the intuition of many paleontologists who argued that the known fossil record for crown groups of bilaterian phyla is largely robust (*11*).

Our divergence estimates suggest that crown-group demosponges (Figs. 1 and 3, dark blue circle) and crown-group cnidarians (yellow circle) have deep origins, both at nearly 700 Ma. These could represent artifacts, although the former is corroborated by Cryogenian-age fossil molecules (biomarkers) of demosponges (*21*) and possible sponge body fossils reported from the Cryogenian (*22*). The deep divergence of the cnidarian crown group is less easily explained, but the degree of molecular divergence among cnidarian classes is roughly equal to the protostome-deuterostome divergence (*23*), which is consistent with our results.

The Neoproterozoic fossil record. The unavoidable conclusion from the molecular record is that precambrian animals are largely stem lineages leading to extant phyla, and that these lineages originated in the Ediacaran (Figs. 1 and

3). Numerous eukaryotic taxa, including the first example of multicellularity with complex development (*24*), are represented in rocks assigned to the later (i.e., <580 Ma) Ediacaran Period. Among these fossils should be organisms that can be unambiguously assigned to the Metazoa and to more inclusive lineages (e.g., Bilateria), but mostly these fossils are enigmatic and lineages with diagnostic bilaterian apomorphies have not been identified.

The Ediacaran-aged Doushantuo Formation of South China has yielded a suite of fossilized, multicellular structures of diverse morphology (Fig. 2F), which have been interpreted by some as the early cleavage states of metazoan embryos (*25*). Although some of these forms have been assigned to bilaterian clades (*26*) or described as metazoan resting stages (*27*), it is likely that few (if any) actually represent crown-group metazoans, especially given the absence of any evidence for gastrulation, a metazoan-specific feature (*28*).

More typical of this age is the Ediacara macrobiota (579 to 541 Ma). Emerging consensus is that these fossils represent multiple independent clades of macroscopic organisms (*29*), to which a new framework for Ediacaran phylog-

eny and classification, highlighting six clades and three likely clades, is proposed (Materials and Methods, SOM text 3, and tables S5 and S6). These clades emphasize a greater amount of higher-order disparity than previously appreciated for these fossils, in contrast to previous analyses that grouped all Ediacara macrofossils as a single extinct clade (*30*) or phylogenetic schemes that emphasize a metazoan-only ancestry (*31*). The proposed framework allows for a direct comparison with higher-order classification in Cambrian metazoans. Three distinct biostratigraphic zones have been recognized (*32*). The Avalon assemblage (579 to ~560 Ma) is largely found in Newfoundland and England. This fauna is dominated by the Rangeomorpha (*33*), a clade (SOM text 3) of modular organisms built from repetitively branched ("fractal") units (Fig. 2G), and it also includes potential macroscopic sponges (*34*). The White Sea assemblage (~560 to ~550 Ma) is widespread and faunally diverse (Fig. 2H) with more than three times the genera of the Avalon assemblage (SOM text 3), marking an expansion in ecospace occupation (*35*) and behavioral complexity as reflected by diverse trace fossils. The youngest assemblage, the Nama (~550 to 541 Ma), is dominated by the Erniettomorpha (Fig. 2I and table S6) and includes evidence of predation in the form of boreholes in the oldest undisputed macroscopic biomineralizing organisms (*36*). Collectively, these three faunas show that assemblages expanded and diversified through the Ediacaran. However, Ediacara macrofossils are not known from the Phanerozoic and evidently went extinct by the Cambrian (*8, 37, 38*).

Aside from putative sponges (*34*), of the nine likely clades of Ediacaran organisms that we recognize (table S6), only two can confidently be assigned to the crown Metazoa. The Kimberellomorpha (Fig. 2H1) are centimeter-sized bilaterally symmetrical fossils with a crenulated margin interpreted as a frill surrounding a muscular foot, and a proboscis (*39, 40*). These bilaterians, and possible molluscs, are commonly associated with radiating trace fossils that may represent feeding on microbial mats (Fig. 2H2). The Dickinsoniomorpha also may have had metazoan affinities. These superficially segmented animals are associated with distinct feeding traces and are possibly stem placozoans or stem eumetazoans (*24, 41*).

Definitive evidence for the presence of bilaterian animals in the Ediacaran comes from surficial trace fossils. Putative trace fossils have been reported from 565 Ma (*42*), but otherwise most are found in rocks <560 Ma (*6, 43*). Trace fossils increase in diversity and complexity toward the Cambrian, when the oldest vertical burrows reveal the presence of a hydrostatically resistant coelom in an organism larger than ~1 cm in diameter. This would seem to provide a strong constraint on the evolution of larger bilaterians (*11, 44*), but the molecular clock ages suggest that coelomic bilaterians (e.g., ambulacrarian
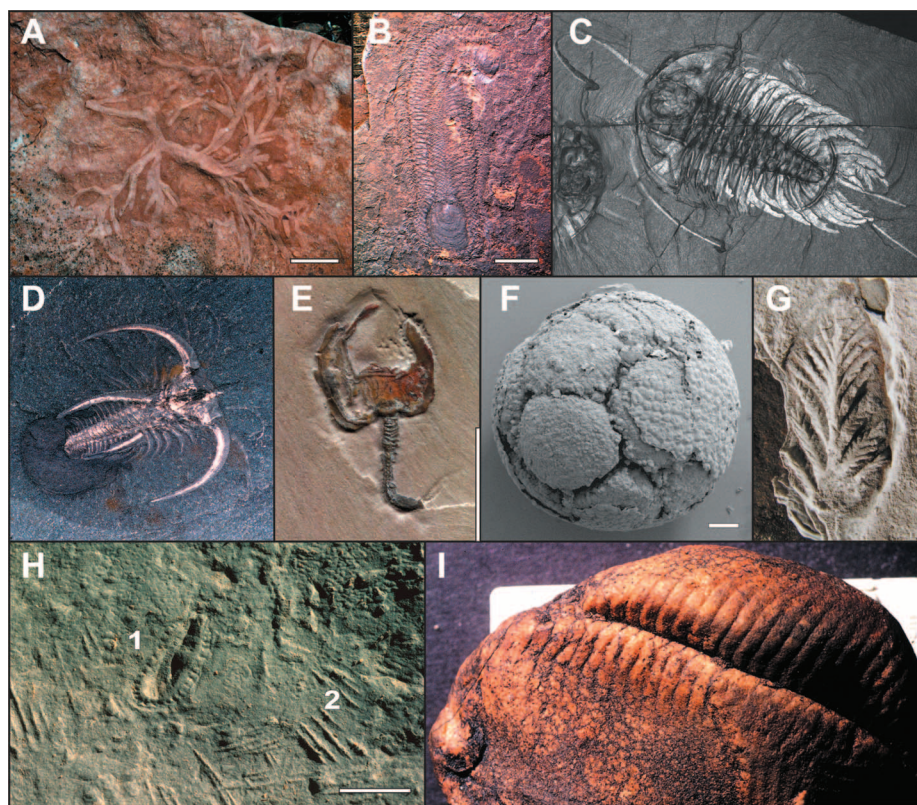

Fig. 2. Fossil diversity during the Ediacaran and Cambrian. (**A**) Early Cambrian complex burrow. (**B**) Scleritome of the small shelly fossil *Halkieria*. (**C**) Mid-Cambrian Burgess Shale trilobite *Olenoides*. (**D**) Stem-group arthropod *Marrella* from the Burgess Shale. (**E**) The stem-group echinoderm *Cothurnocystis* from the mid-Cambrian of Utah. (**F**) Late-stage Doushantuo assemblage of cells (*Tianzhushania*). (**G**) *Avalofractus*, an Ediacaran Rangeomorpha with repetitive branching modularity. (**H**) *Kimberella* (1) with associated *Radulichnus* (2) rasping traces. (**I**) *Pteridinium*, an Ediacaran Erniettomorpha with hollow tubular modular units. Scale bars: (A) 100 μm; (B to I) 1 cm. [Photos: (A), (C), (D), (H), and (I), copyright Smithsonian Institution; (B) provided by J. Vinther; (F) provided by S. Xiao]

deuterostomes) evolved at least 25 million years earlier (Figs. 1 and 3).

In sum, geologic evidence and molecular clock estimates suggest that early animals, notably crown-group demosponges and cnidarians, originated during the Cryogenian. Although bilaterian clades diversified in the Ediacaran, many phylum-level crown groups were not present, appearing first in the Cambrian.

Environmental Potential

Very large geochemical changes have been documented through the Cryogenian and Ediacaran (45–47), which have been interpreted as indicating substantial changes in redox. Changes in molybdenum abundance in black shales (48), the iron chemistry of deep-water sediments (49), and potentially other proxies (46) have been interpreted as a global signal of increased oxygenation during the Ediacaran. The extent to which these signals are truly global, as well as the magnitude of oxidation, remains uncertain. Animals require oxygen to fuel their metabolism, and these geochemical proxies and their interpretation as markers of redox conditions have been invoked to explain the lag between the origin of animals and the Cambrian radiation itself (2). In this view, low oxygen in the oceans and diffusive oxygen transport constrained animals to small size, and only with an increase in oxygen levels could organisms evolve larger, three-dimensional body sizes (24, 50), greatly facilitating their eventual paleontological detection. Thus, although a permissive environment does not explain innovations in metazoan architecture, it might facilitate the appearance of large and ecologically diverse animals in the fossil record.

Genetic and Developmental Possibility

Two findings from comparative genomics and studies of developmental patterning have dramatically changed our understanding of the early evolution of animals. First, whole-genome sequencing of dozens of metazoans has demonstrated that any animal requires only about 20,000 protein-coding genes for the production of its essential morphologic architecture (51). Second, much of this protein-coding repertoire—especially the developmental toolkit—is conserved throughout all metazoans and is even found today among single-celled opisthokonts (24, 52–54). The distribution of these genes in extant organisms (SOM text 3) implies that this toolkit evolved in a two-step pattern (Fig. 4, left): an initial diversification occurring at the base of the Metazoa before the split between sponges and eumetazoans deep in the Cryogenian (and possibly earlier), followed by a pronounced expansion at least in some families at the base of the Eumetazoa during the late Cryogenian (database S3). Thus, the last common ancestor of metazoans, and especially eumetazoans, was a genetically complex animal possessing all of the families of protein-coding genes used during development, save for the potential absence

of *Hox* complex genes (55) needed to build the plethora of morphological structures found throughout the crown group.

Consequently, the morphological simplicity of basal animals, and the great differences in morphology between sponges and arthropods or vertebrates, cannot be due to the absence of these protein-coding gene families but instead must involve differences in the temporal and spatial deployment of these genes and their

regulation. By extension, this includes the construction of developmental gene regulatory networks (dGRNs) specific to particular characters (for example, the gut, heart, or appendages). At the core of these networks are extremely conserved, highly refractory and recursively wired suites of genes that are crucial for the specification of many of the characteristic morphologies of major clades (56, 57), and ultimately defining the "developmental morphospace" (57)
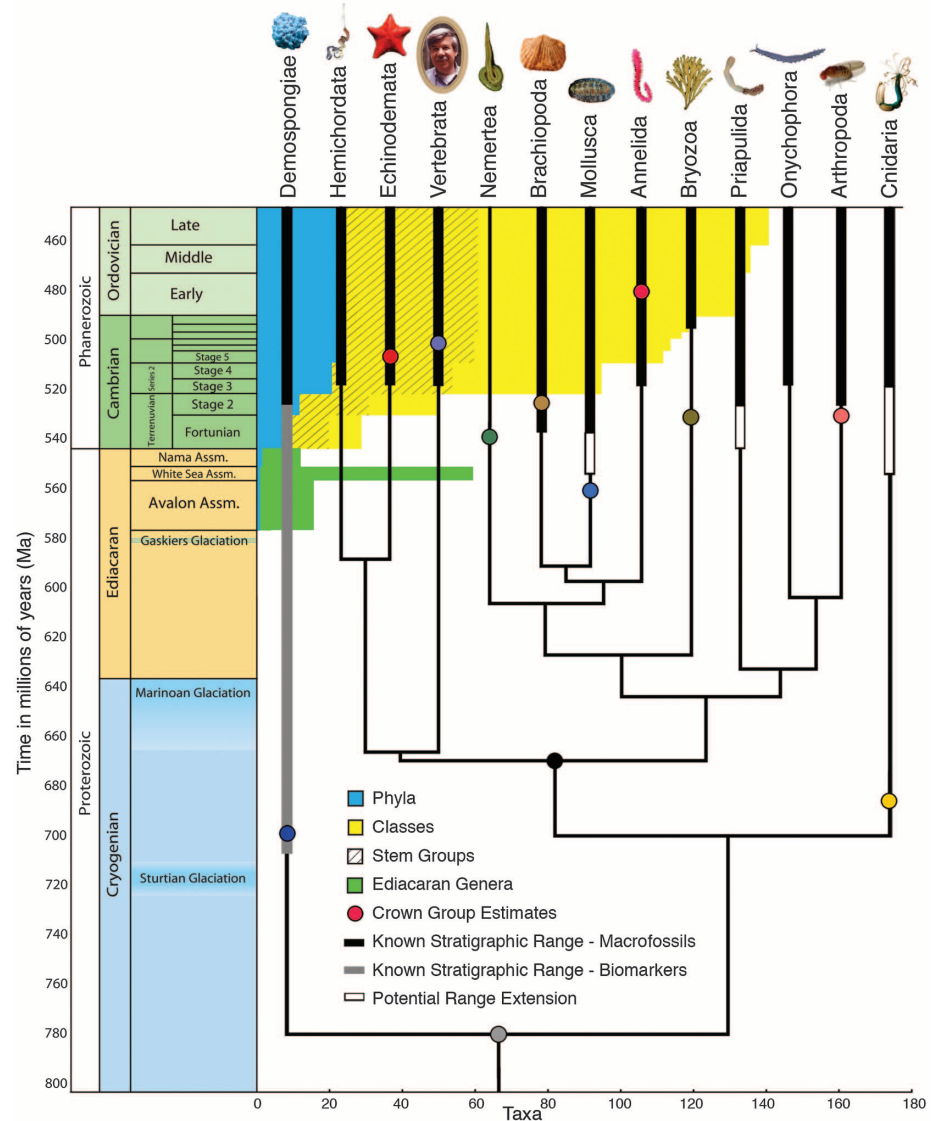

Fig. 3. Detailed stage-level depiction of the animal fossil record as compared to the molecular divergence estimates for 13 different animal lineages. Shown in yellow and blue is the known fossil record of animals at the class and phylum levels, respectively (hatching indicates "stem" lineages, i.e., lineages that belong to a specific phylum but not to any of its living classes); shown in green is the generic record of macroscopic Ediacara fossils (see scale at bottom). Shown in thick black lines are the known fossil records of each of these 13 lineages through the Cryogenian-Ordovician (table S1); most lineages make their first appearance in the Cambrian, consistent with the known fossil record of all animals (yellow and blue). Further, the extent of these stratigraphic ranges closely mirrors the molecular estimates for the age of each of the respective crown groups (colored circles) (see also Fig. 1), highlighting the general accuracy of the molecular clock. Only cnidarians have an unexpectedly deep crown-group origination as estimated by the molecular clock, as the deep demosponge divergence is apparent from taxon-specific biomarkers (gray bar) (21).

accessible to a clade. Such networks are likely to have evolved via intercalary evolution in which developmental genes providing spatial, temporal, and homeostatic control were inserted into preexisting simpler dGRN subcircuits (58). One example of genetic intercalation into these dGRNs is the continual evolutionary addition of micro-RNAs (miRNAs). miRNAs encode ~22-nucleotide noncoding regulatory RNAs that affect the translation of target mRNAs, ultimately contributing to the maintenance of cellular homeostasis and cellular identity (59) and to the robustness of developmental programs (60). Unlike the mRNA toolkit, which was largely established before the evolution of bilaterians (Fig. 4, left), miRNAs (database S4) seem to have been continuously added to eumetazoan genomes through time with very little secondary loss in most taxa (Fig. 4, right) (60). When loss did occur, it seems to have been associated with morphological simplification (20). For example, each of the extant animals put forth as putative biological models for late precambrian animals, including lophotrochozoan flatworms, acoel flatworms, and *Xenoturbella* (61), are characterized by extensive secondary loss of their miRNA complements as compared to more typical invertebrates like ambulacrarian deuterostomes, crustacean arthropods, and polychaete annelids (60). In contrast, large expansions in the number of miRNA families correlate to increases in the number of cell types and mor-

phological complexity of animals, as seen, for example, at the base of the bilaterians and at the base of the vertebrates (60) (Fig. 4, right).

Whereas there is little difference in the mRNA toolkit between humans and sea anemones (Fig. 4, left), there is a dramatic difference in the miRNA toolkit between these two taxa (Fig. 4, right). The increasing morphologic complexity and developmental stability of bilaterian lineages then likely reflects, at least in part, an increase in the diversity and number of dGRN subcircuits, including the continued and hierarchical incorporation of miRNAs into these networks in a lineage-specific manner (60). Other potentially noteworthy aspects of regulatory control that may be important in bilaterian diversification are other forms of RNA regulation, alternative splicing of transcripts (62), and combinatorial control of enhancers, but we lack sufficient comparative data to evaluate their role in the diversification of bilaterian animals. Because the signaling pathways and transcription factors important for bilaterian development first appeared among basal metazoan clades that originated in the Cryogenian, the advent of elements of the metazoan developmental toolkit was a necessary but not sufficient component of the Cambrian explosion. A subtle but critical change from the views of a decade ago is that the primary developmental contribution to the origin of bilaterians lay with the construction and elaboration of patterns of de-

velopmental control (56, 57), not additions to the mRNA developmental toolkit. The temporal lag between the initial construction of these networks and the eventual appearance of bilaterian fossils suggests that the solution to the dilemma of the Cambrian explosion lies not solely with this genomic and developmental potential, but instead must also be found in the ecology of the Cambrian radiation itself.

Ecological Opportunities

Evolutionary radiations are often described as the invasion of "empty" ecological space, but the transition from the Ediacaran to the Cambrian involved far-reaching changes in benthic and neritic ecosystems and the de novo construction of complex metazoan ecological networks (63, 64). Standard models of adaptive radiation (65) involve diversification from a single clade and cannot explain the polyphyletic nature, morphological and ecological breadth, or the extended duration of this event. Rather, we identify a suite of processes that facilitated the construction of biodiversity through positive feedback: ecosystem engineering of the environment, particularly by Cryogenian-Ediacaran sponges and later by burrowing bilaterians, and the formation of new ecological linkages including the evolution of zooplankton, which connected pelagic and benthic systems (64), and the advent of metazoan predation.

Fig. 4. Acquisition and secondary loss of messenger RNAs (mRNAs, **left**) and microRNAs (miRNAs, **right**) in selected taxa. One hundred and thirty-one representative transcription factors and signaling ligands were coded for eight metazoan taxa (database S3) and mapped onto a widely accepted metazoan topology (15, 16). The length of the branch represents the total number of mRNA genes acquired minus those that were lost (scale bar represents 10 genes total). Much of the developmental mRNA toolkit was acquired before the last common ancestor of cnidarians and bilaterians. This is in contrast to the miRNA repertoire that displays extensive gain of miRNAs in the bilaterian stem lineage after it split from cnidarians. All 139 miRNA families known from 22 metazoan species were coded (database S4), and similar to the mRNA figure (left), the length of the branch represents the total number of miRNA genes gained at that point minus those that were secondarily lost (scale bar represents 10 genes total). Increases to morphological complexity are correlated with increases to the miRNA toolkit (60), and secondary simplifications in morphology correlate with a relatively high level of secondary miRNA loss (20).
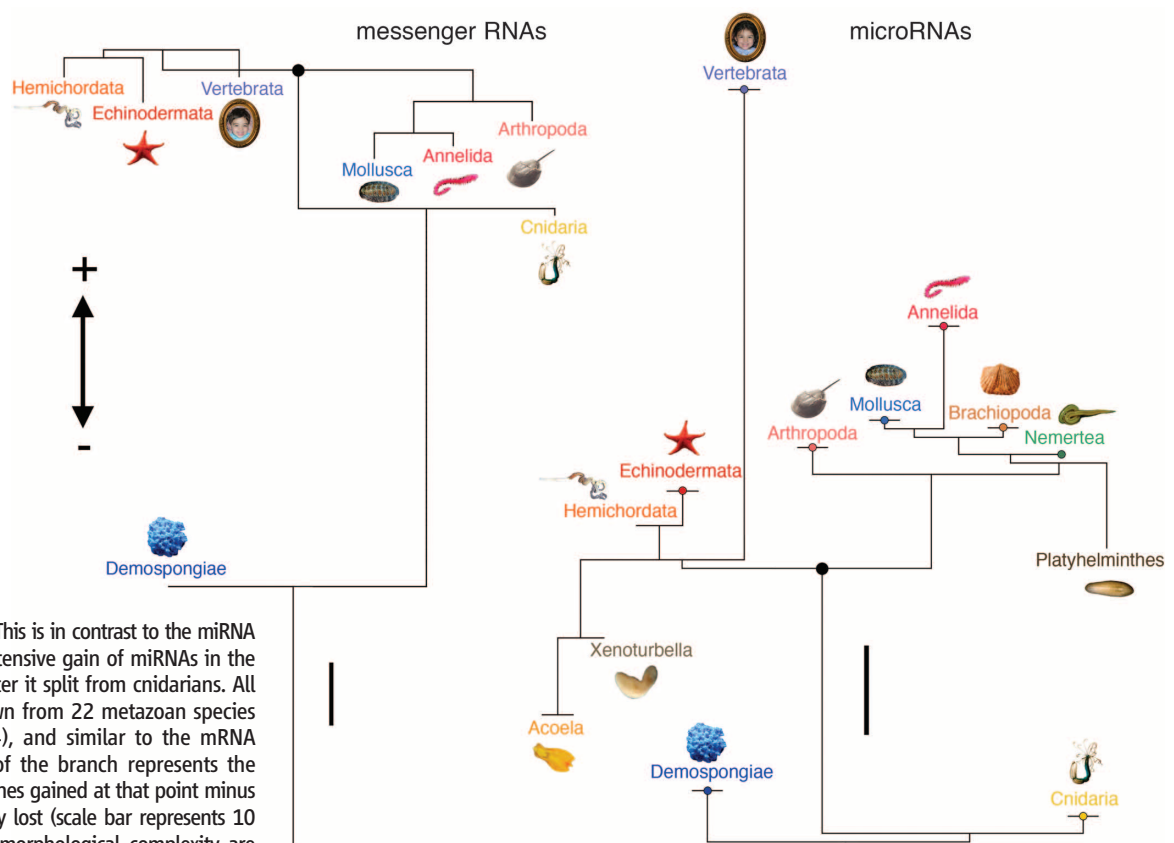
Ecosystem engineering occurs when the activities of one or more species modify the physical and/or chemical environment(s), affecting the flow of energy, nutrients, and other resources through a network of species (66, 67). This often has important ecological and evolutionary consequences (68). The engineering activities with the greatest evolutionary implications are those that affect resource availability. For example, sponges remove dissolved organic matter and bacteria from the water column (34) and when abundant can transfer large volumes of carbon to the sediment, thus changing the geochemistry of the water column. The advent of vertical burrowing in the early Cambrian enhanced the oxygenation of the sediment and microbial primary productivity, providing food for benthic metazoans (69).

Predation was an important component of the growth of these ecological networks. The first appearance of predatory traces, and body fossils of predators, occurs near the Ediacaran-Cambrian transition (70). Animals evolved in response to predation pressures by developing novel defensive mechanisms such as biomineralized shells or developing new structures or capabilities that allowed movement into new habitats. The origin of predation can be assessed by mapping feeding modes onto the time-calibrated phylogeny (Fig. 3). Given the similarities between the sponge feeding cell (choanocyte) and choanoflagellates, the metazoan last common ancestor (LCA) was likely a microphagous suspension feeder, irrespective of whether sponges are monophyletic or not. Cnidarians are potential late Cryogenian predators, and the estimated age of their crown group (~687 Ma) is also the minimal estimate for the evolution of the cnidocyte, the stinging cells that enable cnidarians to prey on other animals. However, the ~150-million-year gap between the appearance of the cnidocyte and the estimated origin of pancrustaceans (Fig. 1), their primary modern prey, raises questions about the nature of early Cryogenian food webs. Cnidarians may have preyed on benthic micro-metazoans, and the correlative innovation of true endomesoderm in bilaterians and the cnidocyte in their immediate sister group, the cnidarians, may suggest a coevolutionary response between these two lineages at this relatively early stage in animal evolution.

Feeding modes along the eumetazoan stem are difficult to polarize (41), but these organisms are unlikely to have been predators, especially upon other animals, as bona fide predation does not appear to be primitive for any of the three great clades of bilaterians. The deuterostome LCA almost certainly filter-fed using gill slits, as the Chordata, Echinodermata, and Hemichordata each have filter-feeding representatives in their basal branches. Within Ecdysozoa, current phylogenetic analyses suggest that the predominantly detritivorous cycloneuralian worms form a paraphyletic assemblage at the base of the clade (71, 72), so detritus feeding was likely primitive for this group. The diversity of feeding strategies among the Lophotrochozoa make it difficult to reconstruct the basal strategy, but because carnivorous molluscs and annelids are derived within each respective phylum, their LCA was unlikely to have been carnivorous either. The only protostome phyla whose crown-group ancestor was likely carnivorous are the chaetognaths and the nemerteans, and both the fossil record (73) and molecular clock results (Fig. 3) suggest that their ancestor appeared in the late Ediacaran to early Cambrian. Thus, we see no evidence for a carnivorous lifestyle during the Cryogenian to mid-Ediacaran for any bilaterian lineage. Given that ecology and the physical environment are closely linked, it may be that the origin of animal carnivory, a metabolically expensive feeding strategy, was driven by increased oxygenation.

Outlook

Our emerging understanding of early animal history shows that evolution is not always relentlessly opportunistic, taking advantage of evolutionary novelties as soon as they arise. Rather, the Cambrian explosion involved the construction of historically unique, and uniquely complex, feedbacks between biological potential and eco-environmental context, including the oxygenation of the ocean's waters. These feedbacks relied on networks of gene regulatory interaction that were established long before the construction of metazoan ecosystems. Because of this long lag between the origin and eventual ecological dominance of clades, data on taxonomic occurrences alone are insufficient to understand evolutionary dynamics and must be accompanied by data on abundances and ecological impact, in addition to accurate and precise estimates of both evolutionary origin and geological first appearances. Macroevolutionary lags such as that which preceded the Cambrian explosion were not unique to animals, as similar dynamics seem to underlie plant evolution as well (24). Understanding both early animal and plant evolution requires an understanding of the processes that generate biodiversity and the expansion of ecological networks through deep time.

References and Notes

1. C. Darwin, *On the Origin of Species by means of Natural Selection* (John Murray, London, 1859).
2. A. H. Knoll, S. B. Carroll, *Science* **284**, 2129 (1999).
3. J. W. Valentine, D. Jablonski, D. H. Erwin, *Development* **126**, 851 (1999).
4. S. A. Bowring et al., *Am. J. Sci.* **307**, 1097 (2007).
5. E. Landing, *Geology* **22**, 179 (1994).
6. S. Jensen, M. L. Droser, J. G. Gehling, in *Neoproterozoic Geobiology and Paleobiology,* S. Xiao, A. J. Kaufman, Eds. (Springer, Berlin, 2006), pp. 115–157.
7. A. C. Maloof et al., *Geol. Soc. Am. Bull.* **122**, 1731 (2010).
8. A. Kouchinsky et al., *Geol. Mag.* 1 (2011).
9. S. M. Porter, *Palaios* **19**, 178 (2004).
10. D. H. Erwin, J. W. Valentine, J. J. Sepkoski Jr., *Evolution* **41**, 1177 (1987).
11. G. E. Budd, S. Jensen, *Biol. Rev. Camb. Philos. Soc.* **75**, 253 (2000).
12. B. Runnegar, *Lethaia* **15**, 199 (1982).
13. K. J. Peterson et al., *Proc. Natl. Acad. Sci. U.S.A.* **101**, 6536 (2004).
14. K. J. Peterson, J. A. Cotton, J. G. Gehling, D. Pisani, *Philos. Trans. R. Soc. Lond. B Biol. Sci.* **363**, 1435 (2008).
15. H. Philippe et al., *Curr. Biol.* **19**, 706 (2009).
16. K. M. Halanych, *Annu. Rev. Ecol. Syst.* **35**, 229 (2004).
17. E. A. Sperling, K. J. Peterson, D. Pisani, *Mol. Biol. Evol.* **26**, 2261 (2009).
18. J. Baguñà, M. Riutort, *Bioessays* **26**, 1046 (2004).
19. A. Hejnol, M. Q. Martindale, *Philos. Trans. R. Soc. Lond. B Biol. Sci.* **363**, 1493 (2008).
20. H. Philippe et al., *Nature* **470**, 255 (2011).
21. G. D. Love et al., *Nature* **457**, 718 (2009).
22. A. C. Maloof et al., *Nat. Geosci.* **3**, 653 (2010).
23. N. H. Putnam et al., *Science* **317**, 86 (2007).
24. A. H. Knoll, *Annu. Rev. Earth Planet. Sci.* **39**, 217 (2011).
25. S. H. Xiao, Y. Zhang, A. H. Knoll, *Nature* **391**, 553 (1998).
26. J. Y. Chen et al., *Science* **305**, 218 (2004).
27. P. A. Cohen, A. H. Knoll, R. B. Kodner, *Proc. Natl. Acad. Sci. U.S.A.* **106**, 6519 (2009).
28. J. W. Hagadorn et al., *Science* **314**, 291 (2006).
29. S. H. Xiao, M. Laflamme, *Trends Ecol. Evol.* **24**, 31 (2009).
30. A. Seilacher, *Lethaia* **22**, 229 (1989).
31. J. G. Gehling, *Mem. Geol. Soc. India* **20**, 181 (1991).
32. B. M. Waggoner, *Integr. Comp. Biol.* **43**, 104 (2003).
33. G. M. Narbonne, *Science* **305**, 1141 (2004).
34. E. A. Sperling, K. J. Peterson, M. Laflamme, *Geobiology* **9**, 24 (2011).
35. A. M. Bush, R. K. Bambach, D. H. Erwin, in *Quantifying the Evolution of Early Life,* M. Laflamme, J. D. Schiffbauer, S. Q. Dornbos, Eds. (Springer Science, 2011), pp. 111–133.
36. S. Bengtson, Y. Zhao, *Science* **257**, 367 (1992).
37. J. E. Amthor et al., *Geology* **31**, 431 (2003).
38. G. M. Narbonne, *Annu. Rev. Earth Planet. Sci.* **33**, 421 (2005).
39. A. Y. Ivantsov, *Paleontol. J.* **43**, 601 (2009).
40. M. A. Fedonkin, A. Simonetta, A. Y. Ivantsov, in *The Rise and Fall of the Ediacaran Biota,* P. Vickers-Rich, P. Komarower, Eds. (Geological Society, London, 2007), pp. 157–179.
41. E. A. Sperling, J. Vinther, *Evol. Dev.* **12**, 201 (2010).
42. A. G. Liu, D. McIlroy, M. D. Brasier, *Geology* **38**, 123 (2010).
43. S. Jensen, M. L. Droser, J. G. Gehling, *Palaeogeogr. Palaeoclimatol. Palaeoecol.* **220**, 19 (2005).
44. J. W. Valentine, D. H. Erwin, in *Development as an Evolutionary Process,* R. A. Raff, Ed. (Liss, New York, 1987).
45. J. P. Grotzinger, D. A. Fike, W. W. Fischer, *Nat. Geosci.* **4**, 285 (2011).
46. G. Shields-Zhou, L. Och, *GSA Today* **21**, 4 (2011).
47. D. A. Fike, J. P. Grotzinger, L. M. Pratt, R. E. Summons, *Nature* **444**, 744 (2006).
48. C. Scott et al., *Nature* **452**, 456 (2008).
49. D. E. Canfield, S. W. Poulton, G. M. Narbonne, *Science* **315**, 92 (2007).
50. B. Runnegar, *Alcheringa* **6**, 223 (1982).
51. D. H. Erwin, *Philos. Trans. R. Soc. Lond. B Biol. Sci.* **364**, 2253 (2009).
52. A. Sebé-Pedrós, A. de Mendoza, B. F. Lang, B. M. Degnan, I. Ruiz-Trillo, *Mol. Biol. Evol.* **28**, 1241 (2011).
53. G. S. Richards, B. M. Degnan, *Cold Spring Harb. Symp. Quant. Biol.* **74**, 81 (2009).
54. M. Srivastava et al., *Nature* **466**, 720 (2010).
55. J. F. Ryan et al., *Genome Biol.* **7**, R64 (2006).
56. E. H. Davidson, D. H. Erwin, *Science* **311**, 796 (2006).
57. E. H. Davidson, D. H. Erwin, *Cold Spring Harb. Symp. Quant. Biol.* **74**, 65 (2009).
58. E. H. Davidson, D. H. Erwin, *J. Exp. Zool. B (Mol. Dev. Evol.)* **314B**, 182 (2010).
59. E. V. Makeyev, T. Maniatis, *Science* **319**, 1789 (2008).
60. K. J. Peterson, M. R. Dietrich, M. A. McPeek, *Bioessays* **31**, 736 (2009).

61. C. R. Marshall, J. W. Valentine, *Evolution* **64**, 1189 (2010).
62. A. Kalsotra, T. A. Cooper, *Nat. Rev. Genet.* **12**, 715 (2011).
63. D. H. Erwin, J. W. Valentine, *The Cambrian Explosion: The Construction of Animal Biodiversity* (Roberts, Greenwood, CO, 2012).
64. N. J. Butterfield, *Paleobiology* **23**, 247 (1997).
65. J. B. Losos, *Am. Nat.* **175**, 623 (2010).
66. C. G. Jones, J. H. Lawton, M. Shachak, *Ecology* **78**, 1946 (1997).
67. J. P. Wright, C. G. Jones, *Bioscience* **56**, 203 (2006).
68. D. H. Erwin, *Trends Ecol. Evol.* **23**, 304 (2008).
69. A. M. Lohrer, S. F. Thrush, M. M. Gibbs, *Nature* **431**, 1092 (2004).
70. S. Bengtson, *Paleontol. Soc. Pap.* **8**, 289 (2002).
71. O. Rota-Stabelli et al., *Proc. R. Soc. B* **278**, 298 (2011).
72. L. I. Campbell et al., *Proc. Natl. Acad. Sci. U.S.A.* **108**, 15920 (2011).
73. H. Szaniawski, *Acta Palaeontol. Pol.* **47**, 409 (2002).

A Potent and Broad Neutralizing Antibody Recognizes and Penetrates the HIV Glycan Shield

Robert Pejchal,[1]* Katie J. Doores,[2,3]* Laura M. Walker,[2]* Reza Khayat,[1]* Po-Ssu Huang,[4]* Sheng-Kai Wang,[5] Robyn L. Stanfield,[1] Jean-Philippe Julien,[1] Alejandra Ramos,[2] Max Crispin,[6] Rafael Depetris,[7] Umesh Katpally,[8] Andre Marozsan,[8] Albert Cupo,[8] Sebastien Maloveste,[9] Yan Liu,[10] Ryan McBride,[11] Yukishige Ito,[12] Rogier W. Sanders,[7,13] Cassandra Ogohara,[4] James C. Paulson,[11] Ten Feizi,[10] Christopher N. Scanlan,[6] Chi-Huey Wong,[5] John P. Moore,[7] William C. Olson,[8] Andrew B. Ward,[1] Pascal Poignard,[2,14] William R. Schief,[2,4] Dennis R. Burton,[2,3]† Ian A. Wilson[1]†

The HIV envelope (Env) protein gp120 is protected from antibody recognition by a dense glycan shield. However, several of the recently identified PGT broadly neutralizing antibodies appear to interact directly with the HIV glycan coat. Crystal structures of antigen-binding fragments (Fabs) PGT 127 and 128 with Man$_9$ at 1.65 and 1.29 angstrom resolution, respectively, and glycan binding data delineate a specific high mannose-binding site. Fab PGT 128 complexed with a fully glycosylated gp120 outer domain at 3.25 angstroms reveals that the antibody penetrates the glycan shield and recognizes two conserved glycans as well as a short β-strand segment of the gp120 V3 loop, accounting for its high binding affinity and broad specificify. Furthermore, our data suggest that the high neutralization potency of PGT 127 and 128 immunoglobulin Gs may be mediated by cross-linking Env trimers on the viral surface.

Viruses have evolved a variety of mechanisms to escape antibody recognition, many of which involve features of the viral surface proteins, such as high variability, steric occlusion, and glycan coating. For HIV, the dense shield of glycans (*1, 2*) that decorate the viral Env protein was once believed to be refractory to antibody recognition, masking conserved functionally significant protein epitopes for which greater exposure would result in increased susceptibility to antibody neutralization. However, the broadly neutralizing monoclonal antibody (bnmAb) 2G12 and several of the recently described PGT antibodies appear to bind directly to the HIV glycan coat. Although carbohydrate-protein interactions are typically weak (*3*), 2G12 recognizes terminal dimannose (Manα1,2Man) moieties on oligomannose glycans, using an unusual domain-exchanged antibody structure that creates a multivalent binding surface that enhances the affinity of the interaction through avidity effects (*4*). However, although 2G12 neutralizes clade B isolates broadly, it is less effective against other clades, particularly clade C viruses, which have a somewhat different oligomannose glycan arrangement than clade B viruses. In contrast, we have recently isolated six bnmAbs (PGTs 125 to 128, 130, and 131) that bind specifically to the Man$_{8/9}$ glycans on gp120 and potently neutralize across clades (*5*). PGT 128, the broadest of these antibodies, neutralizes over 70% of globally circulating viruses and is, on average, an order of magnitude more potent than the recently described PG9, PG16, VRC01, and PGV04 (also known as VRC-PG04) bnmAbs (*5–8*) and is two orders of magnitude more potent than prototype bnmAbs described earlier (*6, 9*).

The neutralization potency exhibited by the PGT class of antibodies suggests that they may provide protection at relatively low serum concentrations. Hence, the epitopes recognized by these antibodies may be good vaccine targets if appropriate immunogens can be designed.

Crystal structures of PGTs 127 and 128 bound to Man$_9$. To gain a structural understanding of the specificity for Man$_{8/9}$ glycans by PGTs 127 and 128, we first determined crystal structures of the Fabs of PGTs 127 and 128 with a synthetic Man$_9$ glycan lacking the core *N*-acetylglucosamine (GlcNAc) moieties at 1.65 and 1.29 Å resolution, respectively (table S1). The bound glycan is well ordered, except for the terminal mannose residue of the D2 arm (Fig. 1 and figs. S1 and S2A). The 127/Man$_9$ and 128/Man$_9$ structures show a similar conformation for the glycan (fig. S1), demonstrating a conserved mode of recognition by these clonally related antibodies.

Analysis of these crystal structures reveals the origin of their specificity for Man$_{8/9}$ glycans. The terminal mannose residues of both the D1 and D3 arms, which are only present on Man$_{8/9}$ glycans (Fig. 1B, Fig. 2A, and fig. S2A), are heavily contacted, forming 11 of the 16 total hydrogen-bonding interactions with the antibody (table S2). This specificity for glycans is consistent with glycan array data showing binding of PGT 127 and 128 to Man$_8$ and Man$_9$, but not to monoglucosylated Man$_9$ N-glycans (fig. S3A), and with glycosidase inhibitor specificity

[1]Department of Molecular Biology, Skaggs Institute for Chemical Biology, and International AIDS Vaccine Initiative (IAVI) Neutralizing Antibody Center, The Scripps Research Institute, La Jolla, CA 92037, USA. [2]Department of Immunology and Microbial Science and IAVI Neutralizing Antibody Center, The Scripps Research Institute, La Jolla, CA 92037, USA. [3]Ragon Institute of MGH, MIT, and Harvard, Cambridge, MA 02129, USA. [4]Department of Biochemistry, University of Washington, Seattle, WA 98195, USA. [5]Department of Chemistry, The Scripps Research Institute, La Jolla, CA 92037, USA. [6]Oxford Glycobiology Institute, Department of Biochemistry, University of Oxford, South Parks Road, Oxford, OX1 3QU, UK. [7]Weill Medical College of Cornell University, New York, NY 10021, USA. [8]Progenics Pharmaceuticals, Tarrytown, NY 10591, USA. [9]Laboratory of Molecular Microbiology, National Institute of Allergy and Infectious Diseases, National Institutes of Health, Bethesda, MD 20892, USA. [10]Glycosciences Laboratory, Department of Medicine, Imperial College London, Hammersmith Campus, Du Cane Road, London, W12 0NN, UK. [11]Department of Physiological Chemistry, The Scripps Research Institute, La Jolla, CA 92037, USA. [12]RIKEN Advanced Science Institute and Exploratory Research for Advanced Technology, Japan Science and Technology Agency, 2-1 Hirosawa, Wako, Saitama 351-0198, Japan. [13]Department of Medical Microbiology, Academic Medical Center, Amsterdam, Netherlands. [14]International AIDS Vaccine Initiative, New York, NY 10038, USA.

*These authors contributed equally to this work.
†To whom correspondence should be addressed: E-mail: burton@scripps.edu (D.R.B.); wilson@scripps.edu (I.A.W.)